
1 This manuscript has been accepted for publication in *Geochemical*
2 *Perspectives Letters* on 27 of March 2024. Please refer to the
3 published manuscript for the final version of the paper.

4
5 Medieval and recent SO₂ budgets in the Reykjanes
6 Peninsula: implication for future hazard

7
8 A. Caracciolo¹, E. Bali¹, E. Ranta², S. A. Halldórsson¹, G. H. Guðfinnsson¹, B. V. Óskarsson³

9
10 (1) NordVulk, Institute of Earth Sciences, University of Iceland, 102, Reykjavík, Iceland.

11 (2) Department of Geosciences and Geography, University of Helsinki, Finland

12 (3) Icelandic Institute of Natural History, Urriðaholsstræti 6–8, Garðabær, 7110, Iceland

13
14 Corresponding author: Alberto Caracciolo (alberto@hi.is)

15

16

17

18

19

20

21 Abstract

22 Exposure to volcanic SO₂ can have adverse effects on human health, with severe respiratory disorders
23 documented on short- and long-term timescales. Here, we use melt inclusion and groundmass glass
24 data to calculate potential syn-eruptive SO₂ emissions during the medieval and the recent 2021-2024
25 eruptions across the Reykjanes peninsula, the most populated area of Iceland that has recently
26 undergone magmatic reactivation with the 2021-2024 eruptions at Fagradalsfjall and Svartsengi. We
27 target 16 individual eruptions from the medieval volcanic cycle at the Reykjanes Peninsula, the 800-
28 1240 AD Fires, along with the 2021-23 Fagradalsfjall eruptions and the 2023-24 eruptions at
29 Sundhnúksgrágar. We calculate potential SO₂ emissions across the RP for the individual eruptions to be
30 in the range 0.004-6.3 Mt. These estimates correspond to mean daily SO₂ emissions in the range 1000-
31 111000 tons/day, higher than the mean SO₂ measurements of 5240 ± 2700 tons/day during the 2021
32 Fagradalsfjall eruption. By using pre-eruptive sulfur values preserved in undegassed melt inclusions,
33 we develop an empirical approach to calculate best- and worst-case potential SO₂ emission scenarios
34 of any past or ongoing RP eruption of known effusion rate. We conclude that the potential sulfur
35 emissions across the RP can be significantly higher than observed during the 2021 Fagradalsfjall
36 eruption, mainly because of the more evolved nature and higher sulfur contents of magmas erupted
37 during the medieval time. Based on dominant NW wind directions on the RP, eruptions in
38 Brennisteinsfjöll pose the greatest health hazard to the capital area. Sulfate aerosol produced during
39 long-term eruptions may impact visibility and air quality in the Keflavík airport area. Our findings
40 enable assessment of SO₂ emission scenarios of future eruptions across the RP and can be used
41 together with gas dispersal models to forecast SO₂ pollution at ground level and its impact on human
42 health.

43

44

45 Introduction

46 The release of volcanic gases and aerosols during volcanic eruptions can significantly impact the air
47 quality and climate (e.g. Ilyinskaya *et al.*, 2017), as well as the biodiversity (e.g., Weiser *et al.*, 2022).
48 Among volcanic gases, sulfur species (SO_2 , H_2S) and associated aerosols (SO_4 , H_2SO_4) are the most
49 critical airborne hazard to human health, with short and long-term impacts that have been recorded
50 at variable distances from eruptive vents (e.g., Horwell *et al.* 2023, Stewart *et al.* 2022; Ilyinskaya *et*
51 *al.*, 2017; Schmidt *et al.*, 2015). For example, several studies have associated cardiorespiratory issues
52 with volcanic sulfur emissions (e.g., Carlsen *et al.*, 2021 and references therein). Hence, a detailed
53 knowledge of potential sulfur releases of active volcanoes located in densely populated areas is critical
54 to understand air quality hazards of future volcanic eruptions. This is the case of the Reykjanes
55 Peninsula (RP) in southwest Iceland, an active spreading area segmented into five volcanic systems,
56 which from west to east are Reykjanes, Svartsengi, Fagradalsfjall, Krýsuvík and Brennisteinsfjöll. The
57 latest magmatic period in the RP occurred ~800 years ago (Sæmundsson *et al.*, 2020) but knowledge
58 about sulfur outputs during those eruptions has been lacking thus far. Each volcanic system on the RP
59 tends to activate during individual magmatic periods (Sæmundsson *et al.*, 2020) and the recent 2021-
60 2024 Fagradalsfjall and Svartsengi eruptions (Barsotti *et al.*, 2023; Sigmundsson *et al.* 2024) suggest
61 the potential initiation of a new eruptive period in an area that hosts ~70% of the Icelandic population.
62 Consequently, there is an increased societal need for a deeper understanding of sulfur emissions
63 across the RP, which is crucial for a comprehensive assessment of sulfur's impact during future
64 eruptions and its potential consequences for human health.

65 Here, we focus on magmatic units erupted in the volcanic systems of Reykjanes, Svartsengi, Krýsuvík
66 and Brennisteinsfjöll in the RP during the last medieval eruptive cycle, which occurred between the 8th
67 century and 1240 AD, hereafter referred to as the 800-1240 AD Fires (Caracciolo *et al.*, 2023; Peate *et*
68 *al.*, 2009). Additionally, we target the 2021-23 Fagradalsfjall eruptions and the December 2023,
69 January 2024 and February 2024 eruptions at Sundhnúksíggar in Svartsengi. We calculate syn-eruptive
70 sulfur release and potential sulfur emissions of 19 geologically and petrochemically well characterized

71 magmatic units (Caracciolo *et al.*, 2023; Peate *et al.*, 2009) and compare those with sulfur emissions
72 from the 2021 Fagradalsfjall eruption (Barsotti *et al.*, 2023; Halldórsson *et al.*, 2022). Also, we estimate
73 daily SO₂ emissions and develop an empirical approach to calculate worst- and best-case potential
74 sulfur emissions for any eruption of a given volume emplaced in the RP.

75 Samples and methods

76 Scoria samples were collected from multiple vents within individual eruptive units of the 800-1240 AD
77 Fires (Caracciolo *et al.*, 2023). Here, we present new sulfur (S) data for the same groundmass glass
78 (n=889) and melt inclusions (MIs) (n=416) dataset published in Caracciolo *et al.* (2023). Additionally,
79 we include new MI and groundmass glass data from the 2022 and 2023 Fagradalsfjall eruptions, as
80 well as data from the eruptions at Sundhnúsgíggar that occurred in the Svartsengi volcanic system in
81 December 2023, January 2024 and February 2024. S was analysed by electron microprobe analyser
82 (EMPA) at the University of Iceland using the same analytical settings as in Caracciolo *et al.* (2020) and
83 MI compositions have been corrected for post-entrapment processes (PEP) (Caracciolo *et al.*, 2023).
84 Here, we use of the ‘petrological method’ (Devine *et al.*, 1984) to calculate eruptive sulfur emissions
85 based on the difference between S concentrations in mineral-hosted MIs and S concentrations
86 measured in groundmass glass (ΔC_S). The idea behind this reconstruction method is that melt
87 inclusions with similar composition to erupted melts preserve the pre-eruptive volatile content, and
88 quenched groundmass glasses provide an estimate of the post-eruptive volatile content. For the
89 different magmatic units, the highest S concentration measured in PEP-corrected MIs ($C_{S\ MI}$) is
90 selected as the pre-eruptive S concentration, whereas the lowest S concentration in groundmass
91 glasses ($C_{S\ glass}$) is chosen as the post-eruptive S concentration. By combining the mass of erupted
92 magmas with the mass of S released, we can assess vent syn-eruptive SO₂ emissions (M_s) of individual
93 eruptions (see Eq. 1 and 2, SOM) (e.g., Bali *et al.*, 2018 and references therein). Furthermore, we
94 calculate the magnitude of potential SO₂ emissions (potential M_s), which refers to complete degassing
95 of all pre-eruptive sulfur ($C_{S\ glass} = 0$) and reflects the maximum amount of SO₂ that a specific eruption

96 could potentially have released, assuming that there is no degassing of unerupted magma. This
97 reconstruction method has been showed to have matched field-based volatile measurements
98 exceptionally well during the 2014-15 Holuhraun eruption (Bali *et al.*, 2018; Pfeffer *et al.*, 2018) and
99 the 2021 Fagradalsfjall eruption (this work, Table 1).

100

101 Sulfur concentrations in MI and groundmass glass

102 Sulfur concentration in MIs is in the range 200-1900 ppm, with a relatively large variability of S at a
103 given MI Mg#. Particularly, the most primitive MIs (Mg#>65), exclusively preserved in Reykjanes and
104 Krýsuvík, record S contents in the range 580-1070 ppm (Fig. 1). S concentration in PEP-corrected MI
105 compositions increases with decreasing MI Mg#, as expected for melt compositions controlled by
106 fractional crystallization. MIs from the 2023-24 eruptions at Sundhnúkgígar record pre-eruptive S
107 concentrations in the range 1400-1600 ppm, in agreement with MI data from the medieval eruptions
108 (Fig. 1b). MIs from the 2022-23 Fagradalsfjall eruptions closely match S concentrations measured in
109 the 2021 products (Fig. 1c). Groundmass glasses from Brennisteinsfjöll have mean S contents in the
110 range 150-280 ppm, lower than mean S contents measured in glasses from the other volcanic systems
111 (280-450 ppm) (Fig. 1, Table 1). For comparison, MIs from the 2021 Fagradalsfjall eruption contain
112 maximum S concentrations of 1200 ppm, whereas the groundmass glasses contain 20-200 ppm S.
113 Sulfide globules were not observed in the erupted samples.

114 Assessing sulfur variability and degassing during the 800-1240 AD

115 Fires

116 Considering that medieval and recent eruptions on the RP are likely sourced from mantle-derived
117 melts of diverse compositions (Caracciolo *et al.*, 2023; Harðardóttir *et al.*, 2022; Halldórsson *et al.*,
118 2022; Peate *et al.*, 2009), including melts with variable S contents (Ranta *et al.*, 2022), we use our MI
119 record to estimate S contents of the local enriched and depleted end-member melt components. We

120 distinguish between these components from the K_2O/TiO_2 variability, a robust tracer of mantle
121 heterogeneities in Iceland (Halldórsson *et al.*, 2022; Harðardóttir *et al.*, 2022) (see SOM). Our
122 modelling, considering that S behaves as an incompatible element in basaltic magmas, shows that
123 most of the MI S variability can be explained by fractional crystallization (FC) and mixing of at least two
124 end-member melt compositions (Fig. 1a-d).

125 In order to evaluate S saturation during magma ascent and fractional crystallization through the crust,
126 we calculate sulfur content at sulfide saturation (SCSS) along a FC path, which reflects the amount of
127 S^{2-} present in a melt in equilibrium with a sulfide phase (Smythe *et al.*, 2017) (see SOM). Our modelling
128 suggests that melts are sulfide undersaturated during most of magmatic fractionation across the RP
129 (Fig. 1 and Fig. S3-S4). Only magmas from Svartsengi and Brennisteinsfjöll have a high likelihood to be
130 sulfide saturated prior to eruptions. Furthermore, sulfide saturation is reached earlier during magmatic
131 differentiation of enriched mantle-derived melts than depleted melts (Fig. 1).

132 Modelling of S degassing with Sulfur_X (Ding *et al.*, 2023) suggests that basaltic melts erupted during
133 the 800-1240 AD Reykjanes Fires are unlikely to degas significant amounts of S at known pre-eruptive
134 magma storage depths (Caracciolo *et al.*, 2023) and that significant S degassing only takes place during
135 magma ascent in the last 0.2 kbar (<700 m) (Fig. S1).

136 Sulfur emissions across the RP

137 Sulfur release ranges between 1000-1770 ppm across the RP, a typical range for Icelandic rift basalts
138 (Ranta *et al.*, 2024), with the largest ΔC_s found in lavas from Svartsengi and Brennisteinsfjöll (Table 1).
139 ΔC_s values can be scaled by the mass of erupted material to estimate M_s of individual eruptions, using
140 published volumes of individual eruptive units, in the range 0.01 km³ to 0.72 km³ (Table 1). Using a
141 melt density of 2700 kg/m³ and assuming a bulk vesicularity of 15 vol%, we calculate M_s between
142 0.003-5.9 Mt (Fig. 2a). The most voluminous lavas found in Svartsengi and Brennisteinsfjöll released
143 the highest mass of SO₂ into the atmosphere during the medieval time. The syn-eruptive SO₂ released
144 by these latter voluminous lavas is approximately 2 to 6 times larger than syn-eruptive SO₂ emissions

145 during the 2021 Fagradalsfjall eruption, for which we estimated $M_s = 0.78$ Mt ($M_{s \text{ measured}} = 0.97 \pm 0.5$,
146 Barsotti *et al.*, 2023). These are roughly between 20 to 70 % of the syn-eruptive SO_2 emissions
147 estimated for the 2014-15 Holuhraun eruption ($M_s = 10.5$ Mt, Bali *et al.*, 2018). We calculate SO_2
148 release of 0.06-0.07 Mt for the 2022 and 2023 Fagradalsfjall eruptions, respectively. However, for a
149 given mass of melt, the 2021-23 Fagradalsfjall eruptions released a comparable mass of SO_2 (Table 1).
150 Oppositely, the 2023-24 eruptions at Sundhnúsgíggar slightly exceeded SO_2 emissions during the 2021-
151 23 Fagradalsfjall eruptions (Table 1). Similarly, we have calculated potential M_s , the maximum mass of
152 SO_2 that could potentially have been released during each eruption. Potential M_s across the RP ranges
153 between 0.003-6.3 Mt and is only slightly higher than vent M_s , as most of the S is released into the
154 atmosphere during eruptions rather than staying dissolved in the lava (Table 1).

155

156 Evaluating end-member scenarios of SO_2 emissions and hazard 157 potential for future eruptions across the RP.

158 Based on the MI record of the 2021-23 Fagradalsfjall eruption (Halldórsson *et al.*, 2022 and this work),
159 the 2023-24 eruptions at Sundhnúsgíggar and the 800-1240 AD Fires (this work), we constrain
160 potential maximum (1900 ppm) and minimum (1170 ppm) pre-eruptive S concentrations and use
161 these to estimate potential M_s of future eruptions in the RP. With these constraints, we developed an
162 empirical approach to assess potential M_s for a given eruption of known lava volume, with important
163 applications for forecasting the worst- and best-case scenarios of potential M_s of future eruptive events
164 (Fig. 2b). For example, based on our approach, an eruption with an eruptive volume of 0.4 km^3 , could
165 release between 2.9 Mt and 4.1 Mt of SO_2 . This method also has an application when it comes
166 evaluating the long-term SO_2 impact of ongoing eruptions in the RP. If the mean magma output rate
167 (MOR) is known and fixed, one can roughly estimate the volume of the lava flow and calculate potential
168 M_s at any given moment from the onset of the eruption. This provides a valuable tool to assess best-
169 and worst-case scenarios for SO_2 pollution during ongoing events.

170 Eruptive M_s calculations are strongly dependent on lava flow volumes. Hence, when it comes to
171 comparing the 800-1240 AD Fires with the 2021-24 eruptions, a more relevant parameter is the mean
172 daily SO_2 emissions, which also is an important parameter from a hazard perspective. We have
173 estimated daily SO_2 emissions for the 800-1240 AD Fires using MOR values calculated by Oskarsson *et*
174 *al.*, (2024), in the range 3-119 m^3/s (Table 1, Eq. 3 SOM). Mean daily SO_2 emissions during the medieval
175 eruptions likely ranged between 1000 ton/day to 111000 ton/day (Fig. 2c). In comparison, during the
176 2021, 2022 and 2023 Fagradalsfjall eruptions, we calculate average daily SO_2 emissions of 5000, 3780
177 and 3360 ton/day, respectively. The estimate for the 2021 Fagradalsfjall eruption is in agreement with
178 the majority of measured daily SO_2 emissions throughout the 2021 Fagradalsfjall eruption, in the range
179 1000-7600 ton/day (Esse *et al.*, 2023), and with daily SO_2 emissions of 5240 ± 2700 ton/day, calculated
180 assuming 0.97 ± 0.5 Mt of total mass of SO_2 (Barsotti *et al.*, 2023). Oppositely, the Dec. 2023
181 Sundhnúkar eruption released 32000 ton/day SO_2 (Table 1). Our calculations highlight that future
182 eruptions in the RP may have the potential to release significantly more SO_2 on a daily basis than the
183 2021-24 eruptions.

184 SO_2 emissions during the 800-1240 AD Fires and the 2021-24 eruptions are small compared to those
185 during the 2014-15 Holuhraun basaltic eruption (9.2 Mt SO_2 , Pfeffer *et al.*, 2018). However, volcanic
186 eruptions in the RP are potentially considered to be more hazardous due to their proximity to
187 inhabited areas, to the international airport and to the large number of visitors expected at eruption
188 sites (Fig. 3) (Barsotti *et al.*, 2023). To assess the health hazard for potential future eruptions, we built
189 seasonal wind roses, for the period 2012-2022, reflecting dominant wind speeds and directions in the
190 RP (Hersbach *et al.*, 2023). We find that most of the time prevailing winds blow towards the NW-NE,
191 suggesting different SO_2 health hazards potential associated with eruptions within different volcanic
192 systems (Fig. 3). The prevalent NW wind blowing direction suggests that volcanic SO_2 emissions could
193 still be disruptive to the Keflavik airport area if there were a long-duration eruption. Even if eruptions
194 in the RP produce little ash, sulfate aerosol in the atmosphere could reduce visibility and air quality
195 (Pattantyus *et al.*, 2018). Eruptions in Brennisteinsfjöll are the most hazardous for Reykjavík, especially

196 in spring and autumn seasons, as SO₂ is likely to be blown towards the capital area. Eruptions in
197 Reykjanes pose minimal hazard as winds tend to blow away from inhabited areas. During assessment
198 of possible eruptive scenarios in the RP, our estimates provide key input parameters to model the
199 release and dispersion of volcanic SO₂ into the atmosphere. Our results can be used to inform SO₂
200 pollution hazard assessments for potential eruptive scenarios and prompt action and mitigation plans
201 during ongoing volcanic crises in the RP.

202

203 **Acknowledgement**

204 This research was financially support by a NordVulk fellowship awarded to AC and by the Icelandic
205 Research Fund (grant 228933-052). We acknowledge support from the [Gosvá project](#), a research
206 programme on the assessment of volcanic hazard risks in Iceland led by the Icelandic Meteorological
207 Office (IMO). SAH acknowledges support from the Icelandic Research Fund (Grant #196139-051). We
208 thank Christoph Kern, two anonymous reviewers, and editor Ambre Luguët for their constructive
209 comments, which significantly improved the quality of the manuscript.

210

211 **Figure Captions**

212

213 **Table 1.** Eruptive units studied in this work and summary of main results. $C_{S_{MI}}$ = pre-eruptive S
214 concentration. $C_{S_{glass}}$ = post-eruptive S concentration. ΔC_S = sulfur emissions at the vent per unit mass
215 of melt, accounting for crystallinity. V_{bulk} = bulk lava volume. V_{DRE} = Vesicle-free lava volume. M_s = Syn-
216 eruptive SO₂ emissions at the vent. Potential M_s = potential SO₂ emissions. MOR = mean output rates
217 Lava volumes for the medieval eruptions are from Einarsson *et al.* (1991), Jónsson (1978) and
218 Sigurgeirsson (2004). ^a Lava volume estimated by assuming a thickness of 5 m, consistent with average
219 thicknesses of lava flows of known volumes with a similar aerial extent. ^b MOR values (within brackets)
220 and uncertainty ranges for the medieval eruptions are from Óskarsson *et al.* (2024). ^c V and MOR from

221 Pedersen *et al.* (2022). ^dV and MOR from Pedersen *et al.* (2024). *Lava volumes for the 2024 eruptions
222 at Sundhnúkgígur are not available at the current stage.

223

224 **Fig. 1.** (a-d) Variation of S contents in groundmass glasses (filled circles) and PEP-corrected MIs (filled
225 triangles) as a function of Mg# [$Mg\# = 100 \cdot Mg / (Mg + Fe^{2+})$, $Fe^{2+} / Fe^{tot} = 0.9$] in samples from the 800-
226 1240 AD Fires, the 2021-2023 Fagradalsfjall eruptions and the 2023-24 eruptions at Sundhnúkgígur.
227 Data from the 2021 Fagradalsfjall eruption are from Halldórsson *et al.* (2022). Red and blue solid lines
228 indicate fractional crystallization paths calculated for a geochemically enriched and depleted initial
229 melt compositions, respectively (see SOM). The black dotted curve indicates SCSS along an empirical
230 fractional crystallization path calculated after Smythe *et al.* (2017), implemented in PySulfSat (Wieser
231 and Gleeson, 2022).

232

233 **Fig. 2.** (a) Variation of vent M_s (b) Magnitude of potential M_s as a function of eruption volume for the
234 800-1240 AD Fires, the 2021-23 Fagradalsfjall eruptions and the 2023 Sundhnúkar eruption. At a given
235 volume, straight lines allow to calculate potential M_s corresponding to maximum and minimum pre-
236 eruptive S concentrations measured across the RP. Inset plot show most common potential M_s across
237 the RP (c) Daily SO_2 emissions are calculated using MOR values and associated uncertainties from
238 Óskarsson *et al.* (2024). Blue histogram indicates measured SO_2 emissions during the 2021
239 Fagradalsfjall eruption (Esse *et al.*, 2023). Data are coloured according to the volcanic system and only
240 lavas with known volumes or MORs are included in the plots.

241

242 **Fig. 3.** Simplified geological map of the RP and lava flows emplaced during the 800 – 1240 AD Fires.
243 The map also illustrates the aerial extent of the 2021 (Pedersen *et al.*, 2022), 2022 (Gunnarson *et al.*,
244 2023) and 2023 (Belart *et al.*, 2023) Fagradalsfjall lavas. Data from the 2023-24 eruptions at
245 Sundhnúkgígur are from the Landmælingar Íslands geoserver (gis.lmi.is/geoserver). When possible,
246 lava flows are coloured according to calculated syn-eruptive SO_2 emissions, ranging from 0.1 to 6 Mt.

247 Orange outlines show urban areas. Numbers reflect the different lava units as listed in table 1.
248 Seasonal wind roses reflect data at 900 mPa (~1000 m a.s.l), which was the most common SO₂ injection
249 altitude during the 2021 Fagradalsfjall eruption (Esse *et al.*, 2023). Spokes indicate the direction the
250 wind is blowing from, and the length of each spoke shows the frequency. Wind data were extracted
251 from ERA5 (Hersbach *et al.*, 2023).

252

253

254

255

256

257

258

259

260

261

262

263

264

265

266

267

268

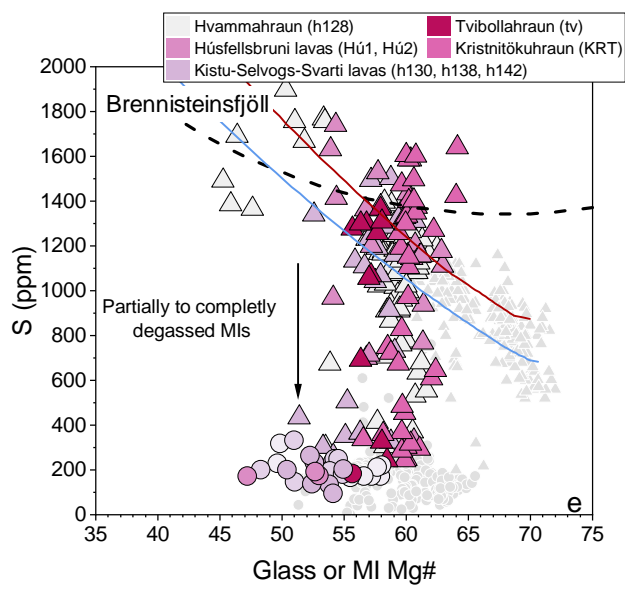
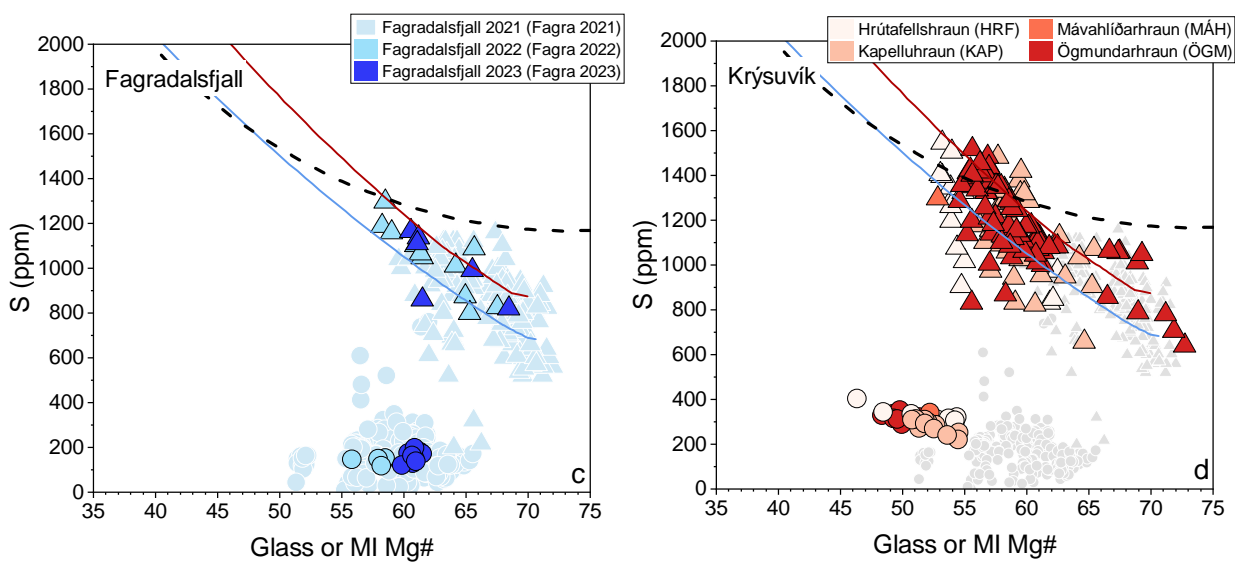
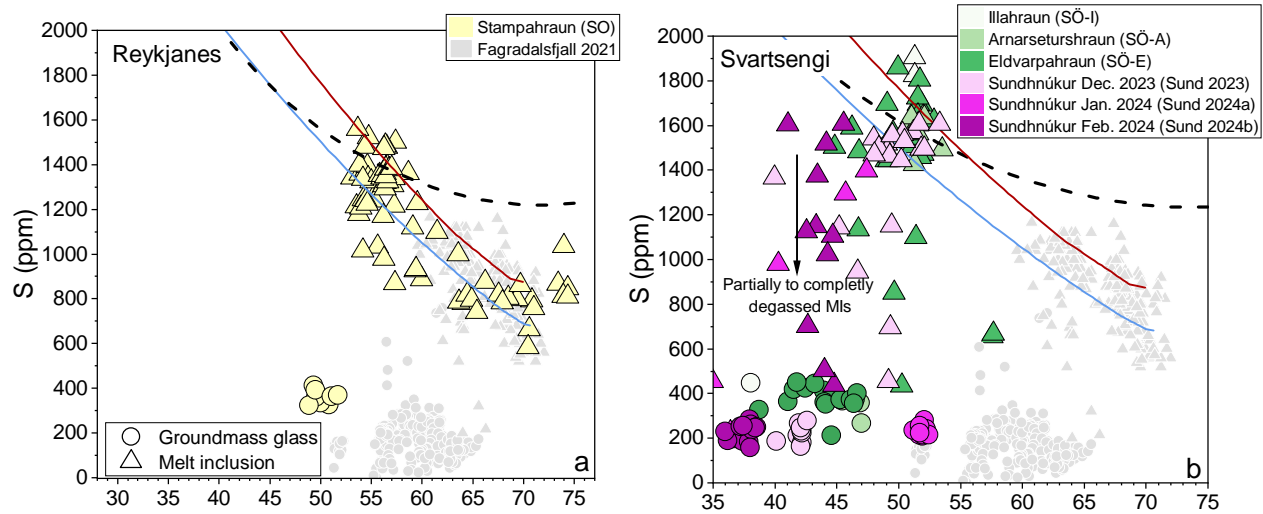
269

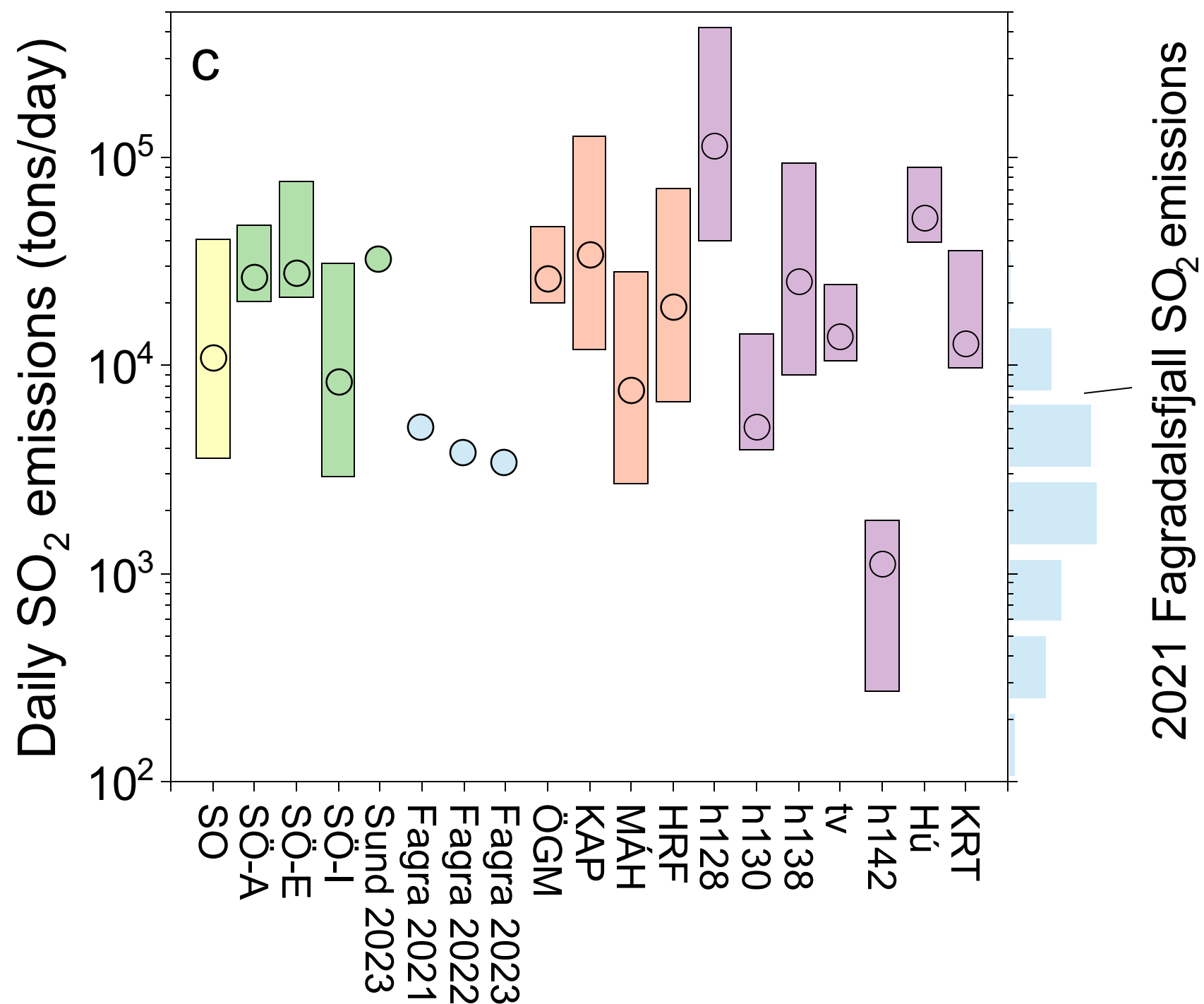
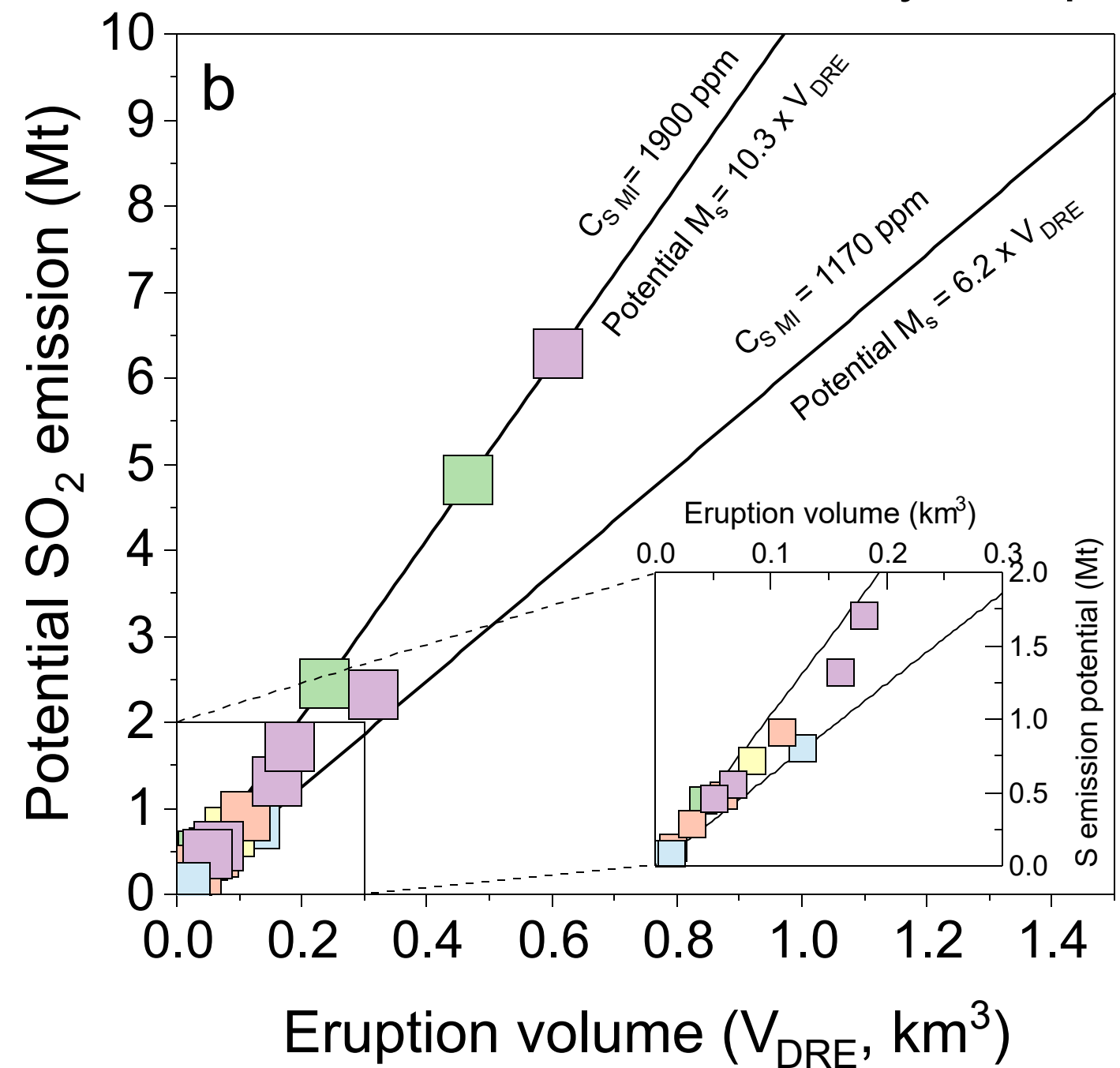
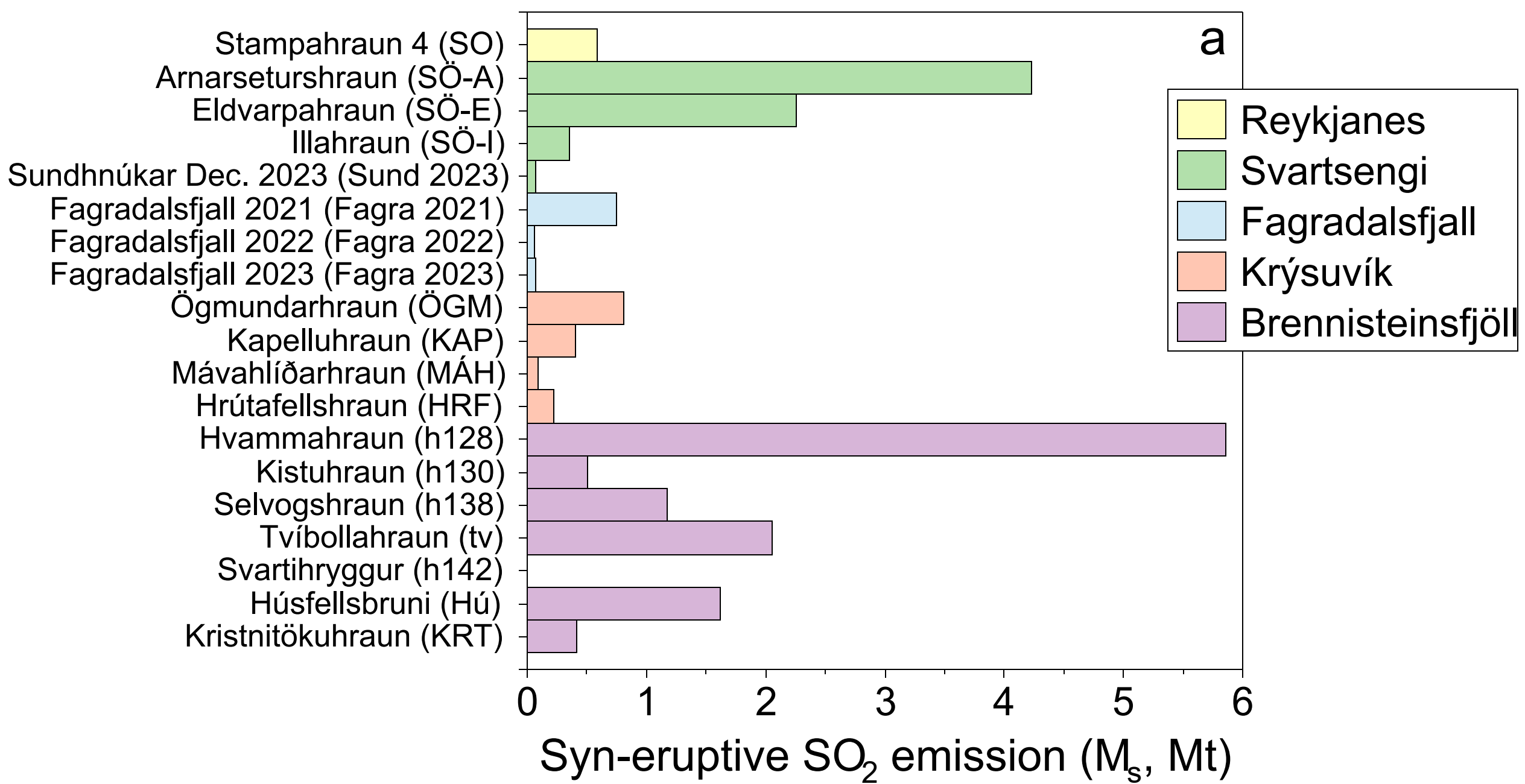
270

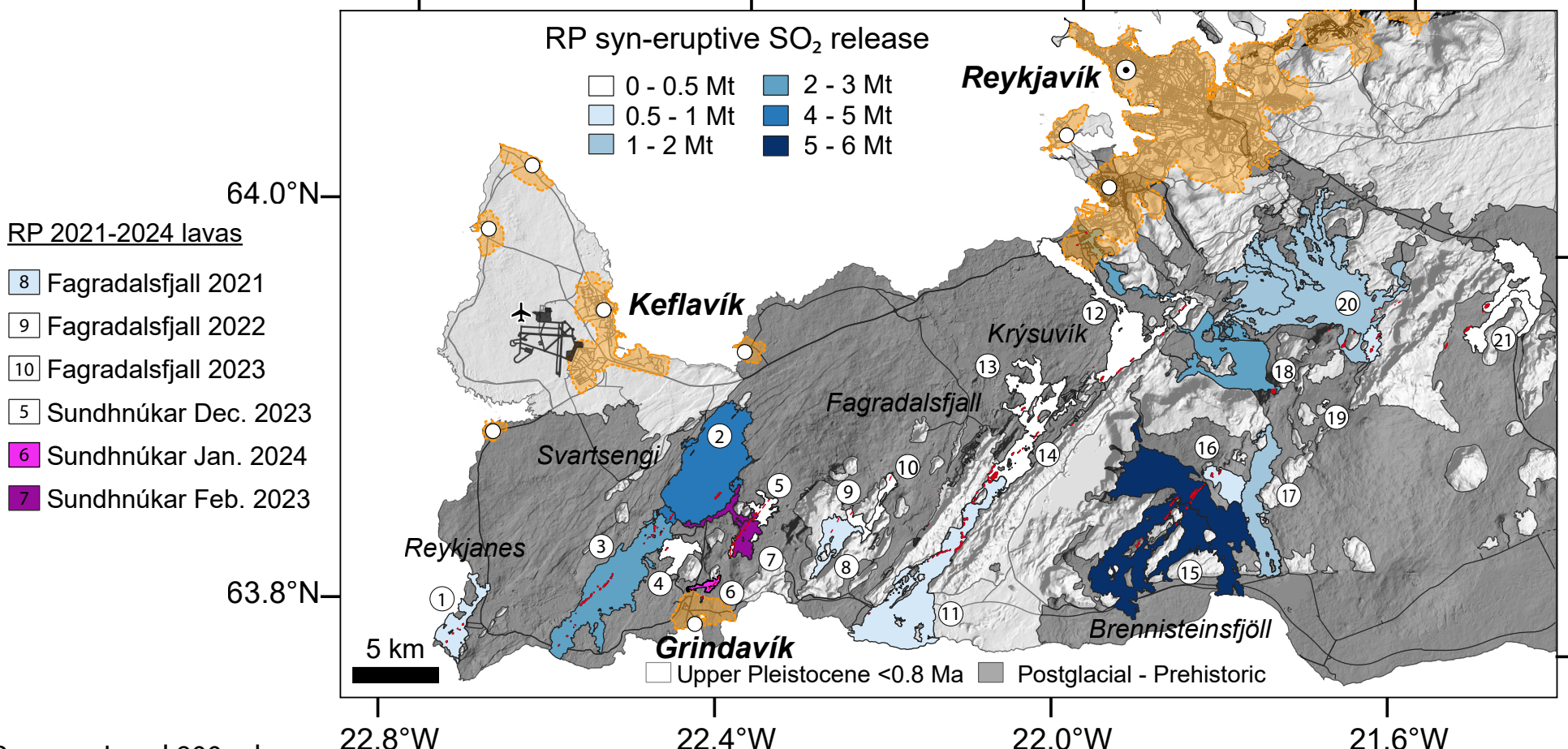
271

272

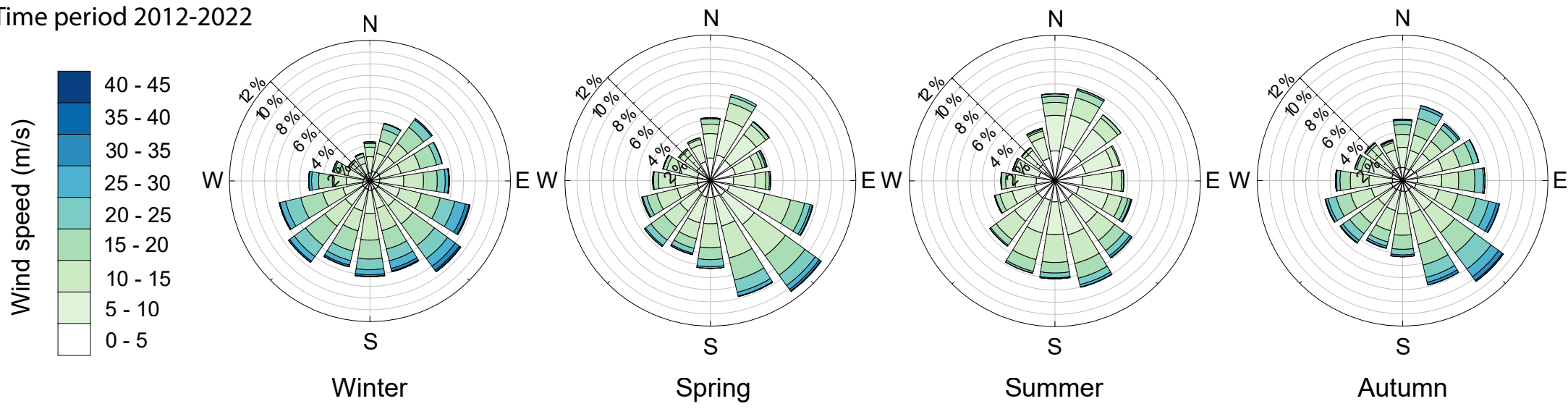
Number	Eruptive unit	Acronym	Volcanic system	Age	C _{S MI}	C _{glass}	ΔC _S	V	V _{DRE}	Mass	M _S	Potential M _S	MOR ^b	Time of lava emplacement	Daily SO ₂ emissions
				A.D.	ppm	ppm	ppm	km ³	km ³	Kg	Mt	Mt	m ³ /s	days	tons/day
1	Stampahraun 4	SO	Reykjanes	1210-1240	1559	258	1275	0.10	0.09	2.3E+11	0.58	0.71	6.4 - 67.9 (17.9)	17 - 193 (65)	3570 - 40450 (10620)
2	Arnarseturshraun	SÓ-A	Svartsengi	1210-1240	1907	196	1667	0.55	0.47	1.3E+12	4.23	4.81	26.1 - 60.1 (33.5)	106 - 244 (190)	20420 - 47000 (26200)
3	Eldvarpahraun	SÓ-E	Svartsengi	1210-1240	1907	112	1759	0.28	0.24	6.4E+11	2.26	2.45	26 - 93.7 (33.3)	35 - 125 (97)	21340 - 76900 (27300)
4	Illahraun	SÓ-I	Svartsengi	1210-1240	1907	312	1563	0.05	0.04	1.1E+11	0.36	0.44	4 - 42.7 (11.2)	14 - 145 (52)	2920 - 31140 (8180)
5	Sundhnúkar Dec. 2023	Sund 2023	Svartsengi	2023	1610	210	1372	0.011 ^d	0.01	2.5E+10	0.07	0.08	50 ^d	2.5	32000
6	Sundhnúkar Jan. 2024*	Sund 2024a	Svartsengi	2024	1400	160	1215	-	-	-	-	-	-	<2	-
7	Sundhnúkar Feb. 2024*	Sund 2024b	Svartsengi	2024	1607	164	1414	-	-	-	-	-	-	<2	-
8	Fagradalsfjall 2021	Fagra 2021	Fagradalsfjall	2021	1170	20	1127	0.15 ^c	0.13	4.1E+11	0.78	0.80	9.5 ^c	185	5000
9	Fagradalsfjall 2022	Fagra 2022	Fagradalsfjall	2022	1300	120	1180	0.011 ^d	0.01	2.5E+10	0.06	0.07	7.0 ^d	18	3780
10	Fagradalsfjall 2023	Fagra 2023	Fagradalsfjall	2023	1170	120	1050	0.015 ^d	0.013	3.4E+10	0.07	0.08	7.0 ^d	26	3360
11	Ögmundarhraun	ÖGM	Krýsuvík	1151-1188	1517	138	1351	0.13	0.11	3.0E+11	0.81	0.90	31.9 - 73.3 (40.8)	21 - 47 (37)	20110 - 46220 (25750)
12	Kapelluhraun	KAP	Krýsuvík	1151-1188	1482	183	1273	0.07	0.06	1.6E+11	0.41	0.48	20.2 - 213 (56)	4 - 40 (14)	12000 - 126500 (33240)
13	Mávahlíðarhraun	MÁH	Krýsuvík	1151-1188	1297	280	997	0.02	0.02	4.6E+10	0.09	0.12	5.8 - 61 (16)	4 - 40 (14)	2700 - 28370 (7450)
14	Hrútafellshraun ^a	HRF	Krýsuvík	8 th - 9 th century	1546	252	1268	0.04 ^a	0.03	9.0E+10	0.23	0.28	11.4 - 120 (31.5)	4 - 40 (14)	6750 - 71000 (18660)
15	Hvammahraun	h128	Brennisteinsfjöll	8 th - 9 th century	1900	90	1810	0.72	0.61	1.7E+12	5.86	6.27	48.3 - 510.6 (134.1)	16 - 173 (62)	39970 - 422560 (111000)
16	Kistuhraun	h130	Brennisteinsfjöll	900-1100	1494	94	1372	0.08	0.07	1.8E+11	0.50	0.55	6.1 - 22 (7.8)	42 - 152 (119)	3900 - 14000 (5000)
17	Selvogshraun	h138	Brennisteinsfjöll	10 th - 11 th century	1504	126	1350	0.19	0.16	4.4E+11	1.18	1.31	14.2 - 149.9 (39.4)	15- 155 (56)	8950 - 94450 (24810)
18	Tvíbollhraun	tv	Brennisteinsfjöll	950	1367	129	1213	0.37	0.31	8.5E+11	2.06	2.32	18.7 - 43 (24)	100 - 229 (178)	10580 - 24340 (13580)
19	Svartihryggur ^a	h142	Brennisteinsfjöll	900-1200	1341	147	1170	0.0005 ^a	0.0004	1.3E+09	0.003	0.003	0.5 - 3.3 (2)	2 - 13 (3)	270 - 1800 (1100)
20	Húsfellsbruni ^a	Hú1 & Hú2	Brennisteinsfjöll	9 - 13 th century	1739	55	1650	0.20 ^a	0.17	4.9E+11	1.62	1.70	50.6 - 116.4 (64.9)	21 - 49 (38)	38960 - 89620 (50000)
21	Kristnitökuhraun ^a	KRT	Brennisteinsfjöll	1000	1640	118	1492	0.06 ^a	0.05	1.4E+11	0.41	0.45	14.1 - 50.9 (18)	14 - 50 (39)	9800 - 35420 (12570)







Pressure Level 900 mbar
Time period 2012-2022



273 References

- 274 Bali, E., Hartley, M.E., Halldórsson, S.A., Gudfinnsson, G.H., Jakobsson, S., (2018). Melt inclusion
275 constraints on volatile systematics and degassing history of the 2014–2015 Holuhraun
276 eruption, Iceland. *Contributions to Mineralogy and Petrology* 173, 9.
277 <https://doi.org/10.1007/s00410-017-1435-0>
- 278 Barsotti, S., Parks, M.M., Pfeffer, M.A., Óladóttir, B.A., Barnie, T., Titos, M.M., Jónsdóttir, K., Pedersen,
279 G.B.M., Hjartardóttir, R., Stefansdóttir, G., Johannsson, T., Arason, Gudmundsson, M.T.,
280 Oddsson, B., Prastarson, R.H., Ófeigsson, B.G., Vogfjörd, K., Geirsson, H., Hjörvar, T., von
281 Löwis, S., Petersen, G.N., Sigurðsson, E.M., (2023). The eruption in Fagradalsfjall (2021,
282 Iceland): how the operational monitoring and the volcanic hazard assessment contributed to
283 its safe access. *Natural Hazards*. <https://doi.org/10.1007/s11069-022-05798-7>
- 284 Belart, J.M.C., Pinel, V., Reynolds, H.I., Berthier, E., Gunnarson, S.R., (2023). Digital Elevation Models
285 (DEMs) and lava outlines from the 2023 Litla-Hrútur eruption, Iceland, from Pléiades satellite
286 stereoimages. Zenodo. <https://doi.org/10.5281/zenodo.10133203>
- 287 Caracciolo, A., Bali, E., Guðfinnsson, G.H., Kahl, M., Halldórsson, S.A., Hartley, M.E., Gunnarsson, H.,
288 (2020). Temporal evolution of magma and crystal mush storage conditions in the
289 Bárðarbunga-Veiðivötn volcanic system, Iceland. *Lithos* 352–353.
290 <https://doi.org/10.1016/j.lithos.2019.105234>
- 291 Caracciolo, A., Bali, E., Halldórsson, S.A., Gudfinnsson, G.H., Kahl, M., Þórðardóttir, I., Pálmadóttir,
292 G.L., Silvestri, V., (2023). Magma plumbing systems and timescale of magmatic processes
293 during historical magmatism on Reykjanes Peninsula. *Earth and Planetary Science Letters*
294 621, 118378. <https://doi.org/10.1016/j.epsl.2023.118378>
- 295 Carlsen, H.K., Valdimarsdóttir, U., Briem, H., Dominici, F., Finnbjörnsdóttir, R.G., Jóhannsson, T.,
296 Aspelund, T., Gislason, T., Gudnason, T., (2021). Severe volcanic SO₂ exposure and

297 respiratory morbidity in the Icelandic population – a register study. *Environmental Health: A*
298 *Global Access Science Source* 20, 1–12. <https://doi.org/10.1186/s12940-021-00698-y>

299 Devine, D., Sigurdsson, H., Davis, A.N., (1984). Estimates of sulfur and chlorine yield to the
300 atmosphere from volcanic eruptions and potential climatic effects. *Journal of Geophysical*
301 *Research* 89, 6309–6325. <https://doi.org/10.1029/JB089iB07p06309>

302 Ding, S., Plank, T., Wallace, P.J., Rasmussen, D.J., (2023). Sulfur_X: A Model of Sulfur Degassing During
303 Magma Ascent. *Geochemistry, Geophysics, Geosystems* 24.
304 <https://doi.org/10.1029/2022GC010552>

305 Einarsson, S., Johannesson, H., Sveinbjörnsdóttir, A.E., (1991). Krísuvíkureldar II. Kapelluhraun og
306 gátan um aldur Hellnahrauns. *Jokull* 41.

307 Esse, B., Burton, M., Hayer, C., Pfeffer, M.A., Barsotti, S., Theys, N., Barnie, T., Titos, M., (2023).
308 Satellite derived SO₂ emissions from the relatively low-intensity, effusive 2021 eruption of
309 Fagradalsfjall, Iceland. *Earth and Planetary Science Letters* 619, 118325.
310 <https://doi.org/10.1016/j.epsl.2023.118325>

311 Fortin, M.A., Riddle, J., Desjardins-Langlais, Y., Baker, D.R., (2015). The effect of water on the sulfur
312 concentration at sulfide saturation (SCSS) in natural melts. *Geochimica et Cosmochimica Acta*
313 160, 100–116. <https://doi.org/10.1016/j.gca.2015.03.022>

314 Gunnarson, S.R., Belart, J.M.C., Óskarsson, B. V., Gudmundsson, M.T., Högnadóttir, T., Pedersen,
315 G.B.M., Dürig, T., Pinel, V., (2023). Automated processing of aerial imagery for geohazards
316 monitoring: Results from Fagradalsfjall eruption, SW Iceland, August 2022. Zenodo.
317 <https://doi.org/10.5281/ZENODO.7871187>

318 Halldórsson, S.A., Marshall, E.W., Caracciolo, A., Matthews, S., Bali, E., Rasmussen, M.B., Ranta, E.,
319 Robin, J.G., Gudfinnsson, G.H., Sigmarsson, O., MacLennan, J., Jackson, M.G., Whitehouse,
320 M.J., Jeon, H., van der Meer, Q.H.A., Mibei, G.K., Kalliokoski, M.H., Repczynska, M.M.,

321 Rúnarsdóttir, R.H., Sigurðsson, G., Pfeffer, M.A., Scott, S.W., Kjartansdóttir, R., Barbara, K.,
322 Kleine, B.I., Oppenheimer, C., Aiuppa, A., Ilyinskaya, E., Bitetto, M., Giudice, G., Stefánsson,
323 A., (2022). Rapid shifting of a deep magmatic source at Fagradalsfjall volcano, Iceland. *Nature*
324 609. <https://doi.org/10.1038/s41586-022-04981-x>

325 Harðardóttir, S., Matthews, S., Halldórsson, S.A., Jackson, M.G., (2022). Spatial distribution and
326 geochemical characterization of Icelandic mantle end-members: Implications for plume
327 geometry and melting processes. *Chemical Geology* 604.
328 <https://doi.org/10.1016/j.chemgeo.2022.120930>

329 Hersbach, H., Bell, B., Berrisford, P., Biavati, G., Horányi, A., Muñoz Sabater, J., Nicolas, J., Peubey, C.,
330 Radu, R., Rozum, I., Schepers, D., Simmons, A., Soci, C., Dee, D., Thépaut, J-N. (2023): ERA5
331 hourly data on pressure levels from 1940 to present. *Copernicus Climate Change Service*
332 (C3S) *Climate Data Store (CDS)*, DOI: [10.24381/cds.bd0915c6](https://doi.org/10.24381/cds.bd0915c6) (Accessed on 26-10-2023)

333 Horwell, C.J., Baxter, P.J., Damby, D.E., Elias, T., Ilyinskaya, E., Sparks, R.S.J., Stewart, C. and Tomasek,
334 I., (2023). The International Volcanic Health Hazard Network (IVHHN): Reflections on twenty
335 years of progress. *Frontiers in Earth Science*, 11, <https://doi.org/10.3389/feart.2023.1213363>

336 Ilyinskaya, E., Schmidt, A., Mather, T.A., Pope, F.D., Witham, C., Baxter, P., Jóhannsson, T., Pfeffer, M.,
337 Barsotti, S., Singh, A., Sanderson, P., Bergsson, B., McCormick Kilbride, B., Donovan, A.,
338 Peters, N., Oppenheimer, C., Edmonds, M., (2017). Understanding the environmental impacts
339 of large fissure eruptions: Aerosol and gas emissions from the 2014–2015 Holuhraun
340 eruption (Iceland). *Earth and Planetary Science Letters* 472, 309–322.
341 <https://doi.org/10.1016/j.epsl.2017.05.025>

342 Jónsson, J., (1978). Jarðfræðikort af Reykjanesskaga : 1. Skýringar við jarðfræðikort 2. *Jarðfræðikort.*
343 *Orkustofnun.*

344 Óskarsson, B. V. , Askew, R. A., Guðmundsson, H. (2024) Assessing the mean output rate (MOR) of
345 past effusive basaltic eruptions - a look at the postglacial volcanism of the Reykjanes
346 Peninsula in Iceland. Preprint. <https://doi.org/10.31223/X5CH68>

347 Pattantyus, A.K., Businger, S., Howell, S.G., (2018). Review of sulfur dioxide to sulfate aerosol
348 chemistry at Kīlauea Volcano, Hawai‘i. *Atmospheric Environment* 185, 262–271.
349 <https://doi.org/10.1016/j.atmosenv.2018.04.055>

350 Peate, D.W., Baker, J.A., Jakobsson, S.P., Waight, T.E., Kent, A.J.R., Grassineau, N. V., Skovgaard, A.C.,
351 (2009). Historic magmatism on the Reykjanes Peninsula, Iceland: A snap-shot of melt
352 generation at a ridge segment. *Contributions to Mineralogy and Petrology* 157, 359–382.
353 <https://doi.org/10.1007/s00410-008-0339-4>

354 Pedersen, G.B.M., Belart, J.M.C., Óskarsson, B.V., Gudmundsson, M.T., Gies, N., Högnadóttir, T.,
355 Hjartardóttir, Á.R., Pinel, V., Berthier, E., Dürig, T., Reynolds, H.I., Hamilton, C.W., Valsson, G.,
356 Einarsson, P., Ben-Yehosua, D., Gunnarsson, A., Oddsson, B., (2022). Volume, Effusion Rate,
357 and Lava Transport During the 2021 Fagradalsfjall Eruption: Results From Near Real-Time
358 Photogrammetric Monitoring. *Geophysical Research Letters* 49, 1–11.
359 <https://doi.org/10.1029/2021GL097125>

360 Pedersen, G. B. M., Belart, J. M. C., Óskarsson, B. V., Gunnarson, S. R., Gudmundsson, M. T., Reynolds,
361 H. I., Valsson, G., Högnadóttir, T., Pinel, V., Parks, M. M., Drouin, V., Askew, R. A., Dürig, T., and
362 Prastarson, R. H, (2024): Volume, effusion rates and lava hazards of the 2021, 2022 and 2023
363 Reykjanes fires: Lessons learned from near real-time photogrammetric monitoring, EGU
364 General Assembly 2024, Vienna, Austria, 14–19 Apr 2024, EGU24-10724, 2024.
365 <https://meetingorganizer.copernicus.org/EGU24/EGU24-10724.html>

366 Pfeffer, M.A., Bergsson, B., Barsotti, S., Stefánsdóttir, G., Galle, B., Arellano, S., Conde, V., Donovan,
367 A., Ilyinskaya, E., Burton, M., Aiuppa, A., Whitty, R.C.W., Simmons, I.C., Arason, P., Jónasdóttir,

368 E.B., Keller, N.S., Yeo, R.F., Arngrímsson, H., Jóhannsson, P., Butwin, M.K., Askew, R.A.,
369 Dumont, S., Von Löwis, S., Ingvarsson, P., La Spina, A., Thomas, H., Prata, F., Grassa, F.,
370 Giudice, G., Stefánsson, A., Marzano, F., Montopoli, M., Mereu, L., (2018). Ground-Based
371 measurements of the 2014-2015 holuhraun volcanic cloud (Iceland). *Geosciences*
372 (Switzerland) 8, 1–25. <https://doi.org/10.3390/geosciences8010029>

373 Ranta, E., Halldórsson, S.A., Óladóttir, B.A., Pfeffer, M.A., Caracciolo, A., Bali, E., Guðfinnsson, G.H.,
374 Kahl, M. and Barsotti, S., (2024). Magmatic Controls on Volcanic Sulfur Emissions at the
375 Iceland Hotspot. Pre-print. <https://doi.org/10.31223/X51102>

376 Sæmundsson, K., Sigurgeirsson, M., Friðleifsson, G.Ó., (2020). Geology and structure of the
377 Reykjanes volcanic system, Iceland. *Journal of Volcanology and Geothermal Research* 391,
378 106501. <https://doi.org/10.1016/j.jvolgeores.2018.11.022>

379 Sigmundsson, F., Parks, M., Geirsson, H., Hooper, A., Drouin, V., Vogfjörd, K.S., Ófeigsson, G., Greiner,
380 S.H.M., Yang, Y., Lanzi, C., Pascale, G.P. De, Jónsdóttir, K., Hreinsdóttir, S., Tolpekin, V.,
381 Friðriksdóttir, H.M., Einarsson, P., Barsotti, S., (2024). Fracturing and tectonic stress drives
382 ultrarapid magma flow into dikes. *Science*, 383, 1228-1235
383 <https://doi.org/10.1126/science.adn2838>

384 Schmidt, A., Leadbetter, S., Theys, N., Carboni, E., Witham, C.S., Stevenson, J.A., Birch, C.E.,
385 Thordarson, T., Turnock, S., Barsotti, S., Delaney, L., Feng, W., Grainger, R.G., Hort, M.C.,
386 Höskuldsson, Á., Ialongo, I., Ilyinskaya, E., Jóhannsson, T., Kenny, P., Mather, T.A., Richards,
387 N.A.D., Shepherd, J., (2015). Satellite detection, long-range transport, and air quality impacts
388 of volcanic sulfur dioxide from the 2014–2015 flood lava eruption at Bárðarbunga (Iceland).
389 *Journal of Geophysical Research: a* 120, 1–17.
390 <https://doi.org/10.1002/2014JC010485.Received>

391 Sigurgeirsson, M.A., (2004). Þáttur úr gossögu Reykjanes. *Náttúrufræðingurinn* 72, 21–28.

392 Smythe, D.J., Wood, B.J., Kiseeva, E.S., (2017). The S content of silicate melts at sulfide saturation:
393 New experiments and a model incorporating the effects of sulfide composition. *American*
394 *Mineralogist* 102, 795–803. <https://doi.org/10.2138/am-2017-5800CCBY>

395 Stewart, C., Damby, D.E., Horwell, C.J., Elias, T., Ilyinskaya, E., Tomašek, I., Longo, B.M., Schmidt, A.,
396 Carlsen, H.K., Mason, E., Baxter, P.J., Cronin, S., Baxter, P.J., (2022). Volcanic air pollution and
397 human health: recent advances and future directions. *Bulletin of Volcanology*, 84, 11.
398 <https://doi.org/10.1007/s00445-021-01513-9>

399 Weiser, F., Baumann, E., Jentsch, A., Medina, F.M., Lu, M., Nogales, M., Beierkuhnlein, C., (2022).
400 Impact of Volcanic Sulfur Emissions on the Pine Forest of La Palma, Spain. *Forests* 13.
401 <https://doi.org/10.3390/f13020299>

402 Wieser, P.E., Gleeson, M., (2022). PySulfSat: An Open-Source Python3 Tool for modelling sulfide and
403 sulfate saturation. *Volcanica*. <https://doi.org/10.30909/vol.06.01.107127>

404